



Published in final edited form as:

Opt Express. 2009 April 27; 17(9): 7688–7693.

Noninvasive label-free imaging of microhemodynamics by optical-resolution photoacoustic microscopy

Song Hu, Konstantin Maslov, and Lihong V. Wang*

Optical Imaging Laboratory, Department of Biomedical Engineering, Washington University in St. Louis, One Brookings Drive, St. Louis, MO 63130, USA

Abstract

In vivo microcirculatory imaging facilitates the fundamental understanding of many major diseases. However, existing techniques generally require invasive procedures or exogenous contrast agents, which perturb the intrinsic physiology of the microcirculation. Here, we report on optical-resolution photoacoustic microscopy (OR-PAM) for noninvasive label-free microcirculatory imaging at cellular levels. For the first time, OR-PAM demonstrates quantification of hemoglobin concentration and oxygenation in single microvessels down to capillaries. Using this technique, we imaged several important yet elusive microhemodynamic activities—including vasomotion and vasodilation—in small animals *in vivo*. OR-PAM enables functional volumetric imaging of the intact microcirculation, thereby providing greatly improved accuracy and versatility for broad biological and clinical applications.

1. Introduction

The microcirculation plays a central role in the regulation of the metabolic, hemodynamic and thermal state of the individual [1]. Many major diseases [2-8] are manifest in the microcirculation before they are clinically evident, which provides a potential early perspective on the origin and progression of such diseases. However, established clinical imaging modalities such as computed tomography (CT), magnetic resonance imaging (MRI), positron emission tomography (PET), and ultrasonography lack the resolution needed for microvascular imaging [9]. Even with iodine contrast, x-ray imaging cannot image single capillaries. Thus, optical microscopy has been widely used to assess the cellular and molecular features of the microcirculation. Intravital microscopy (IVM), for example, is the gold standard for microcirculation studies. It allows quantification of vessel count, diameter, length, density, permeability, and blood flow velocity. Nevertheless, to observe capillaries *in vivo*, IVM generally requires trans-illumination and surgical preparation [10], restricting its application to limited anatomical sites and interfering with the intrinsic microcirculatory function. Additionally, conventional IVM lacks depth resolution that is crucial for extracting the three-dimensional (3D) microvascular morphology. Confocal microscopy [11] and two-photon microscopy [12], noninvasive and possessing excellent depth-sectioning capability, have difficulty in detecting microvessels without exogenous fluorescent agents, which, although having greatly facilitated laboratory research, are still facing challenges in clinical translations [13]. Orthogonal polarization spectral (OPS) imaging permits noninvasive microvascular imaging without the use of fluorescent dyes [14], paving its way to the bedside. However, OPS provides no depth information and lacks the measurement consistency [15] required for longitudinal studies.

*Corresponding author: E-mail: lhwang@biomed.wustl.edu.

To overcome these difficulties, we have developed optical-resolution photoacoustic microscopy (OR-PAM), a noninvasive volumetric microscopy technology capable of detecting the physiologically specific absorption signatures of endogenous chromophores, such as hemoglobin, *in vivo*. The ability to introduce hemoglobin absorption contrast into the optical-resolution microscopy regime leads to an extremely versatile technique for microcirculation studies, without the limitations of fluorescent labeling and invasiveness. Besides the morphological parameters, such as vessel count, diameter, and length, OR-PAM also validates the quantification of important functional parameters, including total hemoglobin concentration (HbT) and hemoglobin oxygen saturation (sO₂) [16,17] down to the capillary level. Multiple attractive features make OR-PAM a valuable tool for microcirculation studies (Table 1), which is demonstrated below by noninvasively monitoring microhemodynamic activities *in vivo*.

2. Methods

Our OR-PAM system employs nearly diffraction-limited optical focusing with bright field illumination to achieve 5- μ m lateral resolution. The axial resolution is calculated to be \sim 15 μ m, based on the transducer bandwidth and the speed of sound in tissue. The cross-sectional scanning (B-scan) rate over a 1-mm distance is \sim 1 frame per second. The detailed system design is described in [18]. Through time-resolved ultrasonic detection and two-dimensional raster scanning along the transverse plane, the OR-PAM system records the complete 3D microvasculature of the tissue, which can be viewed in direct volumetric rendering (Media 1) or maximum amplitude projection (MAP) image (Fig. 1). All experimental animal procedures were carried out in conformance with the laboratory animal protocol approved by the School of Medicine Animal Studies Committee of Washington University in St. Louis.

3. Results and discussion

Vasodilation, an important vessel activity in regulating tissue oxygen delivery, refers to an increase in vessel diameter. In contrast, vasomotion is a periodic oscillation of the vessel diameter and is not a consequence of the heart beat, respiration, or neuronal input [19]. Substantive experimental work has suggested that vasomotion might serve as a protective mechanism under conditions of ischemia and be an important indicator of cardiovascular events [20], but its physiological role and the underlying mechanism remain elusive [21].

To explore vasomotion and vasodilation in response to tissue oxygen variation, first we selected a 1-mm-by-1-mm region in a nude mouse ear. Structural and sO₂ images (Fig. 2) were acquired by a dual-wavelength measurement under systemic normoxia. According to the sO₂ value, we selected an arteriole-venule pair (A1 and V1 in Fig. 2b), which were almost perpendicular to the B-scan direction (marked by the yellow dashed line in Fig. 2b). In this case, the B-scan image delineates the actual vessel cross section.

Then, we repeated the selected B-scan continuously for seventy minutes, during which the physiological state of the animal was switched between systemic hyperoxia and hypoxia (indicated by the red and blue time segments, respectively, in Figs. 3a-c) by alternating the inspired gas between pure oxygen and hypoxic gas (5% O₂, 5% CO₂ and 90% N₂). Vasomotion and vasodilation were clearly exhibited by the diameter oscillation and expansion of the vessel cross section, respectively, in response to the changes in the physiological state (Figs. 3a, b). To provide quantitative analysis, we estimated the vessel diameter by calculating the full width at half maximum (FWHM) value of the blood vessel signal in each B-scan. The time course of the arteriolar diameter change (Fig. 3c and Media 2) and the corresponding Fourier transform analysis (Fig. 3d) show that arteriole A1 had a significant vasomotion under hyperoxia, with an oscillation frequency of \sim 1.6 cycles-per-min (cpm), which is in good agreement with the

observation from a previous invasive study [22]. Compared with arteriole A1, venule V1 had a much weaker vasomotion with a similar oscillation frequency (Figs. 3c, e). To isolate the vasodilation effect, we smoothed out the diameter oscillation due to vasomotion by 60-point moving averaging (Fig. 3c). The smoothed curve clearly suggests a significant increase of $96 \pm 3\%$ in the arteriolar diameter under hypoxia, whereas the change in the venous diameter is as small as $26 \pm 5\%$. Our results, again, are in good agreement with recent work done by scanning laser ophthalmoscopy with the aid of fluorescent particles [23]. The temporal resolution provided by OR-PAM also enabled us to estimate the 10-90% full-scale response time of vasodilation to systemic hypoxia to be ~ 3 minutes.

4. Perspectives

In future studies, quantification of the local metabolic rate of oxygen consumption would be an exciting extension [24]. To this end, we need to measure the vessel diameter, blood oxygenation, and blood flow. The first two parameters are currently measurable with OR-PAM, and the photoacoustic Doppler (PAD) technique has been suggested for blood flow measurement in the microcirculation [25]. One of our future directions is to integrate PAD flow measurement into the OR-PAM system to assess the local metabolic rate at a microscopic level.

Another interesting direction is to combine OR-PAM with other high-resolution imaging tools, such as confocal microscopy and two-photon microscopy, for multi-modality imaging. The fruitful cellular and molecular information provided by them, based on scattering or fluorescence contrast, will be highly complementary.

Acknowledgments

This work was sponsored by National Institutes of Health grants R01 EB000712, R01 NS46214 (Bioengineering Research Partnerships), R01 EB008085, and U54 CA136398 (Network for Translational Research). L.W. has a financial interest in Endra, Inc., which, however, did not support this work.

References and links

1. Stern MD. In vivo evaluation of microcirculation by coherent light scattering. *Nature* 1975;254:56–58. [PubMed: 1113878]
2. Tooke JE. Microvasculature in diabetes. *Cardiovasc Res* 1996;32:764–771. [PubMed: 8915194]
3. Levy BI, Ambrosio G, Pries AR, Struijker-Boudier HA. Microcirculation in hypertension: a new target for treatment? *Circulation* 2001;104:735–740. [PubMed: 11489784]
4. Bongard O, Bounameaux H, Fagrell B. Effects of oxygen inhalation on skin microcirculation in patients with peripheral arterial occlusive disease. *Circulation* 1992;86:878–886. [PubMed: 1516200]
5. McDonald DM, Baluk P. Significance of blood vessel leakiness in cancer. *Cancer Res* 2002;62:5381–5385. [PubMed: 12235011]
6. Kuo L, Davis MJ, Cannon MS, Chilian WM. Pathophysiological Consequences of Atherosclerosis Extend into the Coronary Microcirculation - Restoration of Endothelium-Dependent Responses by L-Arginine. *Circ Res* 1992;70:465–476. [PubMed: 1537085]
7. Hasdai D, Gibbons RJ, Holmes DR Jr, Higano ST, Lerman A. Coronary endothelial dysfunction in humans is associated with myocardial perfusion defects. *Circulation* 1997;96:3390–3395. [PubMed: 9396432]
8. Iadecola C. Neurovascular regulation in the normal brain and in Alzheimer's disease. *Nat Rev Neurosci* 2004;5:347–360. [PubMed: 15100718]
9. McDonald DM, Choyke PL. Imaging of angiogenesis: from microscope to clinic. *Nature Med* 2003;9:713–725. [PubMed: 12778170]

10. Iga AM, Sarkar S, Sales KM, Winslet MC, Seifalian AM. Quantitating therapeutic disruption of tumor blood flow with intravital video microscopy. *Cancer Res* 2006;66:11517–11519. [PubMed: 17178842]
11. Laemmel E, Genet M, Le Goualher G, Perchant A, Le Gargasson JF, Vicaut E. Fibered confocal fluorescence microscopy (Cell-viZio) facilitates extended imaging in the field of microcirculation. A comparison with intravital microscopy. *J Vasc Res* 2004;41:400–411. [PubMed: 15467299]
12. Kleinfeld D, Mitra PP, Helmchen F, Denk W. Fluctuations and stimulus-induced changes in blood flow observed in individual capillaries in layers 2 through 4 of rat neocortex. *Proc Natl Acad Sci USA* 1998;95:15741–15746. [PubMed: 9861040]
13. Pierce MC, Javier DJ, Richards-Kortum R. Optical contrast agents and imaging systems for detection and diagnosis of cancer. *Int J Cancer* 2008;123:1979–1990. [PubMed: 18712733]
14. Groner W, Winkelman JW, Harris AG, Ince C, Bouma GJ, Messmer K, Nadeau RG. Orthogonal polarization spectral imaging: a new method for study of the microcirculation. *Nature Med* 1999;5:1209–1212. [PubMed: 10502828]
15. Bauer A, Kofler S, Thiel M, Eifert S, Christ F. Monitoring of the sublingual microcirculation in cardiac surgery using orthogonal polarization spectral imaging: preliminary results. *Anesthesiology* 2007;107:939–945. [PubMed: 18043062]
16. Zhang HF, Maslov K, Stoica G, Wang LV. Functional photoacoustic microscopy for high-resolution and noninvasive in vivo imaging. *Nature Biotechnol* 2006;24:848–851. [PubMed: 16823374]
17. Zhang HF, Maslov K, Wang LV. In vivo imaging of subcutaneous structures using functional photoacoustic microscopy. *Nature Protoc* 2007;2:797–804. [PubMed: 17446879]
18. Maslov K, Zhang HF, Hu S, Wang LV. Optical-resolution photoacoustic microscopy for in vivo imaging of single capillaries. *Opt Lett* 2008;33:929–931. [PubMed: 18451942]
19. Aalkaer C, Nilsson H. Vasomotion: cellular background for the oscillator and for the synchronization of smooth muscle cells. *Br J Pharmacol* 2005;144:605–616. [PubMed: 15678091]
20. von Mering GO, Arant CB, Wessel TR, McGorray SP, Bairey Merz CN, Sharaf BL, Smith KM, Olson MB, Johnson BD, Sopko G, Handberg E, Pepine CJ, Kerensky RA. Abnormal coronary vasomotion as a prognostic indicator of cardiovascular events in women: results from the National Heart, Lung, and Blood Institute-Sponsored Women's Ischemia Syndrome Evaluation (WISE). *Circulation* 2004;109:722–725. [PubMed: 14970106]
21. Nilsson H, Aalkjaer C. Vasomotion: mechanisms and physiological importance. *Mol Interv* 2003;3:79–89. 51. [PubMed: 14993429]
22. Bertuglia S, Colantuoni A, Coppini G, Intaglietta M. Hypoxia- or hyperoxia-induced changes in arteriolar vasomotion in skeletal muscle microcirculation. *Am J Physiol* 1991;260:H362–372. [PubMed: 1996682]
23. Lorentz K, Zayas-Santiago A, Tummala S, Derwent JJ. Scanning laser ophthalmoscope-particle tracking method to assess blood velocity during hypoxia and hyperoxia. *Adv Exp Med Biol* 2008;614:253–261. [PubMed: 18290336]
24. Wang LV. Prospects of photoacoustic tomography. *Med Phys* 2008;35:5758–5767. [PubMed: 19175133]
25. Fang H, Maslov K, Wang LV. Photoacoustic Doppler effect from flowing small light-absorbing particles. *Phys Rev Lett* 2007;99:184501. [PubMed: 17995411]

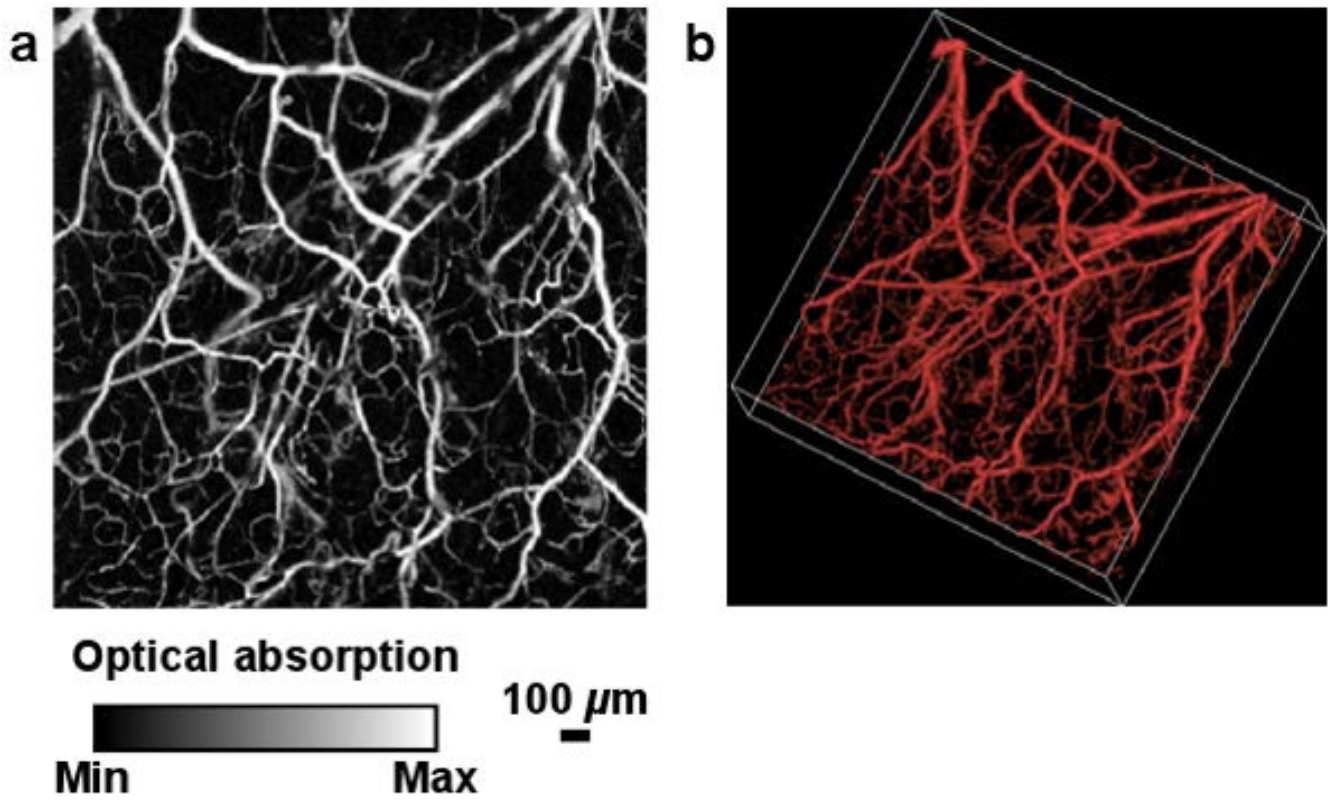


Fig. 1. A representative microvascular network in a nude mouse ear imaged *in vivo* by OR-PAM. (a) MAP image. (b) 3D morphology (Media 1).

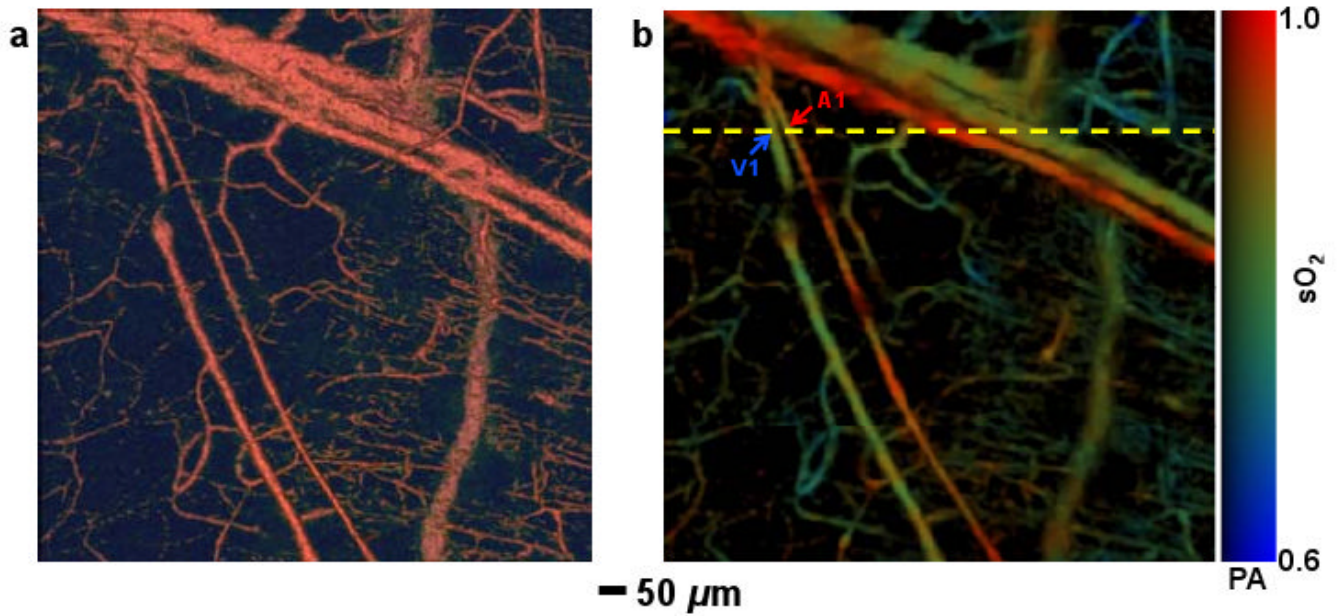


Fig. 2. Structural and functional microvascular imaging by OR-PAM in a nude mouse ear *in vivo*. (a) Structural image acquired at 570 nm. (b) Vessel-by-vessel sO_2 mapping based on dual-wavelength (570 nm and 578 nm) measurements. The calculated sO_2 values are shown in the color bar. PA: photoacoustic signal amplitude. A1: a representative arteriole; V1: a representative venule. Yellow dashed line: the B-scan position for Fig. 3.

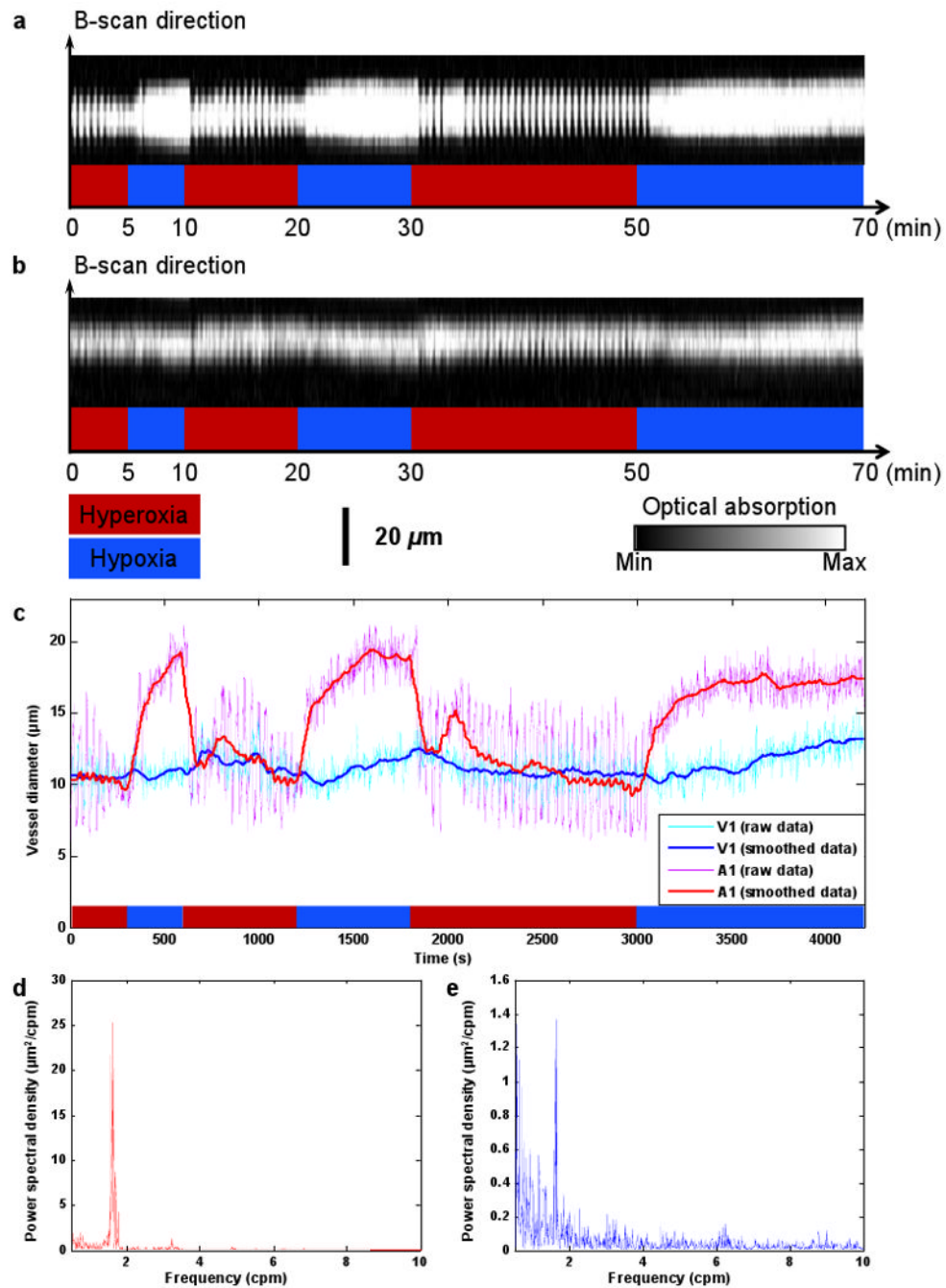


Fig. 3. Vasomotion and vasodilation in response to switching the physiological state between systemic hyperoxia and hypoxia. (a) B-scan monitoring of the changes in the cross section of arteriole A1 (Media 2). (b) B-scan monitoring of the changes in the cross section of venule V1. (c) Changes in arteriolar and venous diameters in response to changes in physiological state (raw data were smoothed via 60-point moving averaging to isolate the effect of vasodilation). (d) Power spectrum of the arteriolar vasomotion tone. (e) Power spectrum of the venous vasomotion tone.

Comparison of modern high-resolution microvascular imaging techniques. CM: confocal microscopy; TPM: two-photon microscopy.

Table 1

Modality	3D morphology	sO ₂ quantification	HbT quantification	Imaging contrast	Working manner
IVM		✓ [†]		Scattering, fluorescence	Invasive
CM	✓			Scattering, fluorescence	Noninvasive
TPM	✓			Fluorescence	Noninvasive
OPS			✓	Absorption [‡]	Noninvasive
OR-PAM	✓	✓	✓	Absorption	Noninvasive

[†]IVM requires adopting Raman spectroscopy for sO₂ measurement.

[‡]Different from OR-PAM, OPS provides negative absorption contrast.